

Intra- and interbrain synchrony and hyperbrain network dynamics of a guitarist quartet and its audience during a concert

Viktor Müller¹ | Ulman Lindenberger^{1,2,3}

¹Center for Lifespan Psychology, Max Planck Institute for Human Development, Berlin, Germany

²Max Planck UCL Centre for Computational Psychiatry and Ageing Research, London, UK

³Max Planck UCL Centre for Computational Psychiatry and Ageing Research, Berlin, Germany

Correspondence

Viktor Müller, Center for Lifespan Psychology, Max Planck Institute for Human Development, Lentzeallee 94, 14195 Berlin, Germany.
Email: vmueller@mpib-berlin.mpg.de

Funding information

Max-Planck-Gesellschaft

Abstract

Playing music in a concert represents a multilevel interaction between musicians and the audience, where interbrain synchronization might play an essential role. Here, we simultaneously recorded electroencephalographs (EEGs) from the brains of eight people during a concert: a quartet of professional guitarists and four participants in the audience. Using phase synchronization analyses between EEG signals within and between brains, we constructed hyperbrain networks, comprising synchronized brain activity across the eight brains, and analyzed them using a graph-theoretical approach. We found that strengths within and between brains in the delta band were higher in the quartet than in the public. Within-brain strengths were higher and between-brain strengths were lower in the music than in the applause condition, both particularly in the quartet group. These changes in coupling strength were accompanied by corresponding changes in the hyperbrain network topology, which were also frequency-specific. Moreover, the network topology and the dynamical structure of guitar sounds showed specific guitar–brain, guitar–guitar, and brain–brain directional associations, indicating multilevel dynamics with upward and downward causation. Finally, the hyperbrain networks exhibit modular structures that were more stable during music performance than during applause. Our findings illustrate complex hyperbrain network interactions in a quartet and its audience during a concert.

KEYWORDS

EEG hyperscanning, graph-theoretical approach, hyperbrain networks, intra- and interbrain coupling, phase synchronization, social interaction

INTRODUCTION

Making music in a concert represents a social interaction in which the musicians communicate with each other and with their audience. This communication is mainly nonverbal and includes different kind of movements, gestures, facial expressions, eye contact, and so on.^{1–5} Hyperscanning experiments have shown that the communication,

at least between the musicians, also takes place on the neural level, which leads to a certain synchronization between the brains. Such communication/coordination is also supported/enhanced by such between-brain synchronization.^{3,6–15} However, the neural mechanisms of such communication and between-brain interaction remain elusive, especially when the interaction involves a group of more than two people/brains.^{14,16–21} The complexity of multibrain dynamics involved

This is an open access article under the terms of the [Creative Commons Attribution](https://creativecommons.org/licenses/by/4.0/) License, which permits use, distribution and reproduction in any medium, provided the original work is properly cited.

© 2023 The Authors. *Annals of the New York Academy of Sciences* published by Wiley Periodicals LLC on behalf of New York Academy of Sciences.

in group interaction has been particularly clearly demonstrated in a study with a quartet of guitarists.¹³ Specific interbrain or rather hyperbrain connectivity structures were shown to emerge during such an interaction. The most intriguing aspect of these structures is that each brain always has to communicate with three other brains and, therefore, develops different configurations depending on the interaction conditions.¹³ In the current study, we examine neural group dynamics between eight brains, with two types or two groups of interaction: four guitarists playing in a quartet and four audience members, representing active and passive interactions, respectively. Since we study two different situations during the concert, namely, the music performance and the applause, active and passive interactions alternate between the groups, with the audience becoming active during the applause and the musicians being rather passive in this case. We expected that active interaction would increase the coupling strength compared to the passive form. In electroencephalographic (EEG) hyperscanning studies, it has been shown that the increase in interbrain synchrony in the audience during live music compared to baseline was dependent on emotional pleasure and closeness²² as well as on the number of people sharing the pleasure and its strength.²³ The same pleasure and a corresponding increase in the interbrain synchrony can also be expected in the musicians, especially during applause. It is well known that hand clapping as an audience expression of appreciation for a good musical performance functions as a social self-organizing system that mostly exhibits specific dynamics with different phases (e.g., fast clapping, synchronization, and slipping back to the fast clapping) and corresponds to the trade-off between optimal synchronization and maximal applause intensity.^{20,24,25} However, the neural mechanisms of clapping or applause remain unexplored. Thus, related to our previous study of the same guitarist quartet, which revealed complex hyperbrain network (HBN) interactions,¹³ this study aims to demonstrate how the HBN structure extends to the audience and how musician and audience components of this structure communicate with each other during two different situations during a concert.

Previous research on neural synchrony in musical interaction has shown that intra- and interbrain synchronization is particularly enhanced during periods that put high demands on musical coordination.^{7,9-13,15} Moreover, it has been shown that there is a specific coupling between musicians' brains and musical instruments.^{8,10,11,26} In this context, it can be expected that such coupling may also occur between audience members' brains and the instruments. However, this should not substantiate the claim that synchronization between brains is simply a result of a common perceptual input and/or a common motor output (cf. Ref. 19). As recently shown in a hyperscanning study of piano duets, keeping sensory input and movements comparable across conditions as well as during musical pauses without sensory input or movement, interbrain synchrony does not merely depend on shared sensorimotor impact but can also emerge endogenously, from aligned cognitive processes supporting social interaction.⁸ Nevertheless, this relationship between brains and instruments provides important evidence that interbrain synchrony has a specific reference to the behavioral actions of musicians (cf. Refs. 9, 10, and 19).

It is also well known that music is generally self-similar, whereby structure and repetition are general features of nearly all music. The concept of self-similarity in music is fundamental for capturing structural properties of music recordings and is provided by the self-similarity matrix (SSM) approach.²⁷ The repetition blocks in SSM resemble each other with respect to certain aspects, such as melody, harmony, or rhythm. Through such recurring patterns, a temporal relationship is established within the piece that can be traced by the listener and evoke a sense of familiarity and musical understanding. Here, we use this concept to investigate the relationships between musical and brain structures in their dynamic interdependency.

Finally, a number of studies have shown that HBNs, comprising intra- and interbrain connectivity, exhibit specific modular organization during music playing and that the most important characteristic of this organization is the existence of so-called hyperbrain modules sharing electrodes or nodes from two or more brains, with strong connections or information flow within the modules and weak connections or information flow between the modules.^{11-13,15} In a previous guitar quartet study, the HBN consisting of four guitarists' brains was shown to be a dynamic structure with nonstationary coupling dynamics and network architecture.¹³ Such networks are highly adaptive to external situations requiring different network states. Moreover, Müller et al.¹⁹ suggested a hyperbrain cell assembly hypothesis that states that cell assemblies can be formed not only within but also between brains, following roughly the same rules as within brains. The hyperbrain cell assembly, comprising the within- and between-brain connections, can lead to the joint firing of neuronal elements in these brains or in the common HBN or cell assembly. It has also been suggested that the hyperbrain module or community can be considered as a prototype of such a hyperbrain cell assembly and that this assembly should gain precedence during repeated joint activity.¹⁹ In this context, it was hypothesized that HBNs comprising eight brains of quartet and audience members would exhibit modular organization, with hyperbrain modules or communities sharing nodes in several brains. Since musical performance is more structured than applause, it was assumed that the modular organization of the HBNs during musical performance would be more stable and less variable in their temporal dynamics than during applause.

MATERIALS AND METHODS

Participants

A quartet of professional guitarists (Cuarteto Apasionado, Berlin) and four listeners in the audience participated in the concert study involving hyperscanning EEG measurement. All participants (females) were right-handed. The guitarists of the quartet (aged between 44 and 48 years, $M = 46.5$, $SD = 1.7$) had been playing the guitar professionally for more than 35 years (mean = 37.8 years, $SD = 1.3$). The audience participants (aged between 20 and 29 years, $M = 22.8$, $SD = 4.2$) were either musically naïve (did not play any instrument, participants F and H) or had taken guitar lessons and played guitar for about 15 years

(participants E and G). Audience members E and G were familiar with each other and also knew the members of the quartet. Participants F and H were not acquainted with anyone. We only recorded four participants from the audience, as we wanted to keep the number of musicians and listeners equal with respect to common network analyses. The Ethics Committee of the Max Planck Institute for Human Development approved the study, and it was performed in accordance with the ethical standards laid down in the 1964 Declaration of Helsinki. All participants volunteered for this experiment and gave their written informed consent prior to their inclusion in the study.

Procedure and data acquisition and analysis

The concert study took place in the auditorium of the Max Planck Institute for Human Development with an audience of more than 150 people (see Figure S1 and Video S1 for details). The program of the concert consisted of eight different pieces of music for classical guitar by different composers and a bonus piece (the program of the concert can be found in the [Supplementary Materials](#)). For analyses, we used three music pieces: M1, "Alguna Calle Gris" from "5 Piezas Artesanales" by Maximo Diego Pujol; M2, "Danza Ritual del Fuego" by Manuel De Falla; and M3, "Säbeltanz" by Aram Chatschaturjan (MP3 files of these pieces of music can be found in the [Supplementary Materials](#)). The concert lasted about 1 h in total. The hyperscanning EEG was simultaneously recorded using eight electrode caps with 28 Ag/AgCl EEG active electrodes each, placed according to the international 10-10 system, with the reference electrode at the right mastoid. The vertical and horizontal electrooculogram was recorded to control for eye blinks and eye movements. The sampling rate of the signals was 5000 Hz. The recorded frequency bands ranged from 0.01 to 1000 Hz. Through one microphone (McCrypt MC-18, Conrad Electronic GmbH, Germany) each, the sounds of the guitars were recorded on four ExG channels, simultaneously with the EEG recordings (BrainAmps MR and BrainAmps ExG, Brain Products, Gilching, Germany). In addition, video and sound were recorded using Video Recorder Software (Brain Products), synchronized with EEG data acquisition. The data were rereferenced offline to an average of the left and right mastoid separately for each participant. Eye movement correction was accomplished by independent component analysis (ICA).²⁸ The average number of removed ICA components was 8.6 (2.0) across participants. Thereafter, artifacts from head and body movements were rejected by visual inspection. Preprocessing of the EEG data (e.g., artifact correction and rejection) was performed using Brain Vision Analyzer 2.2 (Brain Products). The EEG was resampled at 1000 Hz and divided into 20-s epochs indicating different sequences of interest (SOIs). Three SOIs in each music piece and three SOIs during the applause, free of artifacts for all eight participants, were analyzed in terms of intra- and interbrain synchronization. For these purposes, the SOIs were band-pass filtered (using an elliptic infinite impulse response filter) within the four frequency bands: delta (0.5–4 Hz), theta (4–8 Hz), alpha (8–14 Hz), and beta (14–30 Hz). Thereafter, the fast Hilbert transform was applied to extract the phase of the signals in the given frequency bands, which were used for the calculation of phase

synchronization by means of the Phase Synchronization Index (PSI). The PSI was determined by the formula:

$$PSI(f_j) = \left| \left\langle e^{j\Delta\Phi^k(f_j)} \right\rangle \right|, j = \sqrt{-1}, \quad (1)$$

where $\Delta\Phi^k = \text{mod}(\Phi_m^k(f_j) - \Phi_n^k(f_j), 2\pi)$ is the phase difference at the central frequency f_j between the instantaneous phases of the two signals m and n across k data points in the segment; $\Phi_m^k(f_j) = \arg\{y_m^k(f_j)\}$ and $\Phi_n^k(f_j) = \arg\{y_n^k(f_j)\}$. Within the SOI, PSI was calculated using a moving time window of 2000 ms width and a 200-ms time delay between all electrode pairs of all participants (224 × 224). Overall, 91 time windows related to the corresponding SOI were collected by this shifting procedure. Phase synchronization analyses and following network analyses were performed using the NI LabVIEW software (National Instruments, Austin, TX, USA).

Network construction and graph-theoretical approach measures

A graph-theoretical approach (GTA) was used to investigate HBN connectivity on the level of network topology, allowing a systemic view of neural processes within and between the eight brains. For this purpose, we constructed HBNs, including all possible connections within and between the eight brains. In order to remove noisy or spurious connectivity links and emphasize key topological properties of the network, a threshold has to be applied to the connectivity matrix. In general, the choice of the threshold plays an important and nontrivial role in network construction, but is necessarily always arbitrary. At least two issues appear important for us in this study: (1) the connectivity measures should not occur by chance, and (2) the networks changing in time should have the same connection density (a similar number of links), providing a high sparsity level and economical network properties.

In order to fulfill the two criteria, we set the cost level to 20%, which allows for the investigation of sparse economical networks, whereby the connectivity threshold was always higher than the significance level determined by the surrogate data procedure, that is, networks at this cost or sparsity level always included significant connections and had the same number of edges (see [Supplementary Materials](#) for details). This allowed a more accurate examination of the network topology in the different musical pieces and musical sequences or SOIs.

Network and statistical analysis

The aforementioned cost level of 20% was applied to the common HBN, including all electrodes of all eight brains (224 nodes in total) in the quartet (QUA) and in the public audience (PUB). To examine the HBN topology, we determined within- and between-brain strengths (SwB and SbB , respectively), the clustering coefficient (CC), characteristic path length (CPL), local efficiency (E_{local}), and global efficiency (E_{global}). The SwB for node i was calculated as a sum of weights to this node from all other nodes within the particular brain and the SbB for node i in the HBN was calculated as a sum of weights to this

node from all other nodes in all other brains. All other HBN topology measures were calculated based on all nodes in the HBN (see [Supplementary Materials](#) for more details). Thus, the *SbB* reflects the connectivity strength between a particular brain and all other brains, and the other topology measures (*CC*, *CPL*, *E_{local}*, and *E_{global}*) indicate the HBN topology of different nodes/brains within the common HBN. These measures were first determined for each time window and each node in the network and then averaged across all time windows and across nodes divided into the five brain sites separately for each participant/brain: frontal (F: Fp1, Fp2, F3, Fz, F4, FC1, and FC2), central (C: C3, Cz, C4, CP1, and CP2), parietal (P: P3, Pz, P4, O1, Oz, and O2), left-temporal (LT: F7, FC5, T7, TP9, CP5, P7, and PO9), and right-temporal (RT: F8, FC6, T8, TP10, CP6, P8, and PO10). For statistical analysis, GTA measures were averaged across the SOIs of music pieces (MU) and applause (AP). Using a three-way repeated measures ANOVA with a between-subject factor Group (QUA vs. PUB) and within-subject factors Condition (MU vs. AP) and Site (F, C, P, LT, and RT), we separately tested the six GTA metrics across the four frequency bands.

Besides the *common* HBN analyses, comprising nodes from all eight brains, we also conducted *dual* HBN analyses based on all possible pairwise combinations (28 in total) between all quartet and public audience participants. There were six quartet–quartet (Q–Q), six public–public (P–P), and 16 quartet–public (Q–P) pairs, or HBNs with 56 nodes each (see [Figure 1A,B](#) for details). One can see that in contrast to the *common* HBN analyses, we can differentiate the impact of different connection types (i.e., Q–Q, Q–P, and P–P) here. For each of these dual HBNs, we determined the same network topology measures: *SwB*, *SbB*, *CC*, *CPL*, *E_{local}*, and *E_{global}*. All these measures were determined for each time window and node, and then prepared similarly as above. The data were analyzed using a three-way repeated measures ANOVA with a between-subject factor Group (Q–Q, P–P, and Q–P) and a within-subject factors Condition (MU vs. AP) and Site (F, C, P, LT, and RT). When necessary, Greenhouse–Geisser epsilons were applied in all ANOVAs for nonsphericity correction. The Scheffé test was employed for the post-hoc testing of group differences. All statistical analyses were carried out using IBM SPSS Statistics 23.0 (SPSS Inc., Chicago, IL, USA).

Furthermore, we investigated the relationships between guitar sounds and the common HBN topology indices. For these purposes, we first calculated the root mean square of the guitar signals and then constructed self-similarity matrices for each of the guitar sounds by using the moving window approach, just as this was used for the calculation of the connectivity and topology indices in the case of EEG signals (2-s time windows and 200-ms time delay), and subsequently calculated the cosine similarity between all consecutive time windows (91 in total). This results in a 91×91 SSM, reflecting the musical structure of the sound produced during playing. Thereafter, we applied a threshold to the SSM that allowed 20% of the strongest similarity values, and calculated the average strength of each of the nodes in the given SSM, all of which together represent the *similarity profile* or *music structure dynamics* (MSD) and have the same time course as the EEG network topology measures. To investigate the relationships between MSD and network topology dynamics (NTD),²⁹ we calculated (1) Pearson's product correlation (*R*), reflecting linear relationships between the signals, and (2) multivariate Granger causality (*GC*), indicating causal or

directional associations between the signals. For this calculation, five brain regions and three music pieces with the three SOIs each were collapsed together, thus providing a cascade-shaped time series of 4095 data points. The MSD time series were prepared in the same way. *R* and *GC* were determined for the four topology measures in the delta frequency band: *SwB*, *SbB*, *E_{local}*, and *E_{global}*. We limited our analyses to these four topology measures because the *E_{local}* and *E_{global}* represent network topology properties that are relatively similar to *CC* and *CPL*, but unlike the last, are equidirectional. The delta band was chosen because it was only here that the between-brain connections showed significant differences between groups and conditions. In addition to MSD–NTD relationships, MSD–MSD and NTD–NTD were also captured by *R* and *GC* indices. The same analyses were then performed with individual music pieces comprising only 1365 data points.

Finally, we investigated the modular organization of the common HBN and its dynamics across different time windows and SOIs. For these purposes, we determined community structures of the common HBN at each time window in all SOIs of the three music pieces and the applause using the modularity optimization method,^{30,31} which is implemented in the Brain Connectivity Toolbox (<https://sites.google.com/site/bctnet/>; cf. Ref. 32). Modularity of the community structures, a statistic that quantifies the degree to which the network may be subdivided into clearly delineated groups or modules, was thereby assessed. Normalized mutual information (*MI*) between the community structures in the three music pieces and the applause condition was then calculated for clusterings comparison (see [Supplementary Materials](#) for details).^{33,34} The determined *MI* values, which were calculated between each time window and all other time windows in a piece, were organized in a corresponding similarity matrix representing a dynamic stability of modular organization across time. The *MI* values between the community structures in one time window and all others (a row in the similarity matrix) were averaged, indicating the similarity of the community structures of each time window to all others. Resulting similarity values in the three music and applause conditions as well as corresponding modularity values were statistically evaluated by a paired t-test with Bonferroni corrections.

RESULTS

Common HBN topology

Results of the ANOVAs for the six GTA metrics across the four frequency bands are collated in [Table 1](#) and [Figures 2](#) and [3](#). The most significant differences, besides the factor Site, which indicates topology variation across different electrode sites, were found for the factor Condition and its interaction with the factor Group. The main effect Group was significant only for the three GTA measures (*SbB*, *CPL*, and *E_{global}*) in the delta band, whereby *SbB* and *E_{global}* were higher and *CPL* correspondingly shorter in QUA than in PUB (see [Figure 2](#) for details). Interestingly, *SwB* was higher and *SbB* was lower in the MU as compared to the AP condition, both above all in the QUA group. In addition, the *CPL* was shorter during AP than during MU, especially in the QUA group and particularly at the frontocentral and left-temporal sites

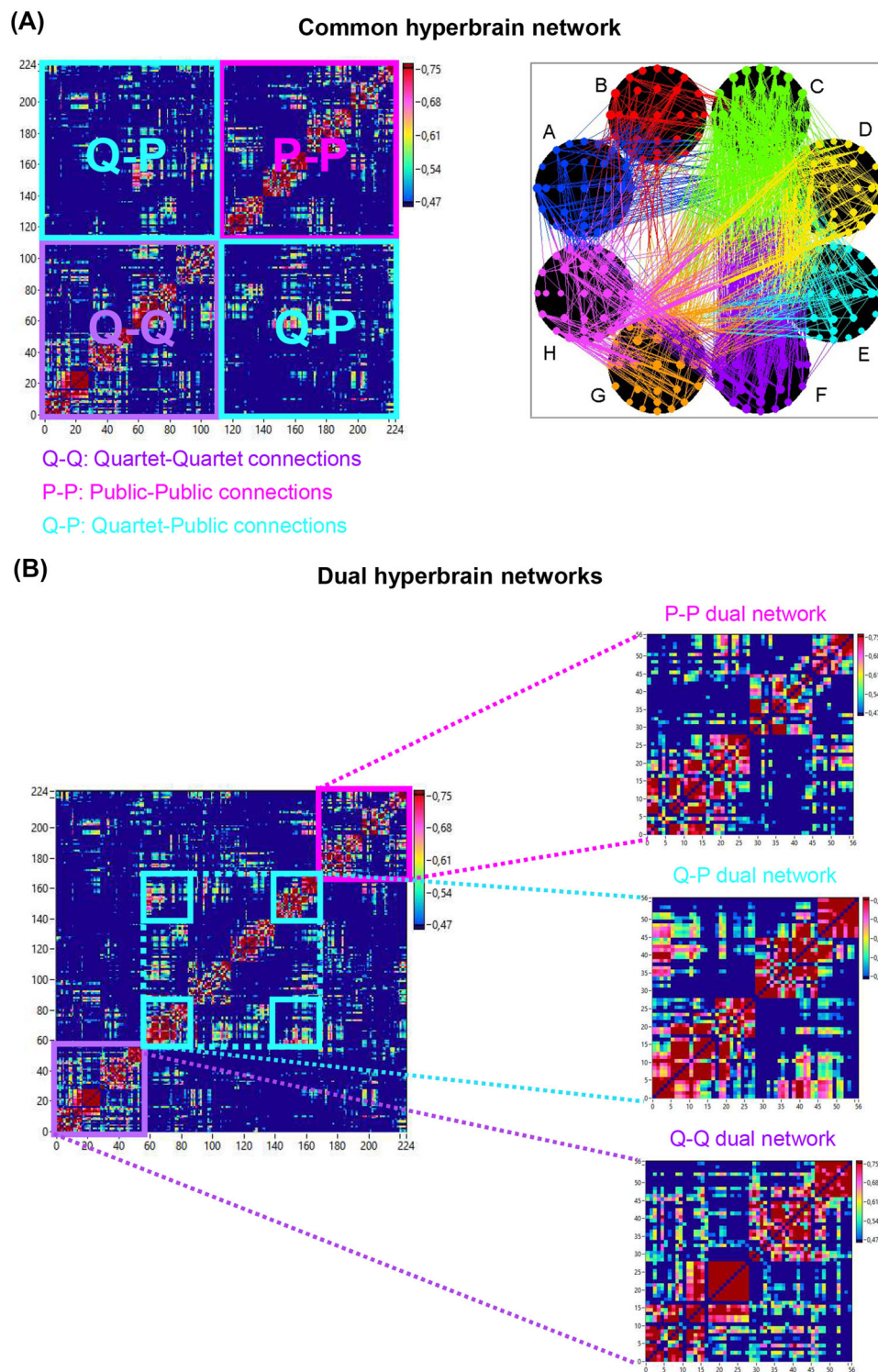


FIGURE 1 Exemplary representation of the common and dual HBNs. (A) Common HBN in the form of the HBN matrix and interbrain connectivity map. In the matrix, including all electrodes of all eight brains (224 nodes in total), different types of links or edges are indicated: Q-Q, quartet-quartet; P-P, public-public; and Q-P, quartet-public. In the connectivity map, the nodes and links of the eight different brains are indicated by color. The guitarists' brains are denoted A, B, C, and D; audience members' brains are denoted E, F, G, and H. (B) Common HBN and three exemplary dual HBNs. On the left, the same common HBN as in panel A is displayed. On the right, three exemplary dual HBNs are presented: P-P dual HBN; Q-P dual HBN; and Q-Q dual HBN. As demonstrated, the dual HBNs constitute certain components of the common HBN. In the heatmaps, the PSI values are indicated by color.

TABLE 1 Significant ANOVA results for the common hyperbrain network indices across the four frequency bands.

Factors	DF	Delta		Theta		Alpha		Beta	
		F value	η^2	F value	η^2	F value	η^2	F value	η^2
<i>SwB</i>									
G	1,6	n.s.		n.s.		n.s.		n.s.	
C	1,6	22.39***	0.79	10.22*	0.63	7.47*	0.55		
S	4,24	12.09***	0.67	16.19***	0.73	12.59***	0.68	10.08**	0.63
G × C	1,6	n.s.		7.41*	0.55	8.40*	0.58	n.s.	
<i>SbB</i>									
G	1,6	410.38***	0.99	n.s.		n.s.		n.s.	
C	1,6	11.11*	0.65	n.s.		n.s.		n.s.	
S	4,24	4.40*	0.42	n.s.		n.s.		n.s.	
G × C	1,6	8.59*	0.59	n.s.		n.s.		8.86*	0.60
<i>CC</i>									
G	1,6	n.s.		n.s.		n.s.		n.s.	
C	1,6	n.s.		44.12***	0.88	19.39***	0.76	n.s.	
S	4,24	5.81*	0.49	7.47**	0.55	7.26**	0.55	9.36**	0.61
G × C	1,6	n.s.		9.83*	0.62	10.01*	0.63	7.44*	0.55
<i>CPL</i>									
G	1,6	21.99**	0.79	n.s.		n.s.		n.s.	
C	1,6	14.13**	0.70	n.s.		n.s.		n.s.	
S	4,24	9.66***	0.62	18.28***	0.75	11.29***	0.65	6.13*	0.51
G × C × S	4,24	3.68*	0.38			n.s.		n.s.	
<i>E_{local}</i>									
G	1,6	n.s.		n.s.		n.s.		n.s.	
C	1,6	n.s.		41.29***	0.87	21.14**	0.78	n.s.	
S	4,24	8.65**	0.59	9.22**	0.61	8.53**	0.59	9.71**	0.62
G × C	1,6	n.s.		9.47*	0.61	10.70*	0.64	7.52*	0.56
<i>E_{global}</i>									
G	1,6	35.38***	0.86	n.s.		n.s.		n.s.	
C	1,6	n.s.		n.s.		n.s.		n.s.	
S	4,24	9.54***	0.61	22.04***	0.79	14.44***	0.71	9.05**	0.60

Abbreviations: C, Condition; CC, clustering coefficient; CPL, characteristic path length; DF, degrees of freedom; E_{global} , global efficiency; E_{local} , local efficiency; G, Group; n.s., nonsignificant; S, Site; *SbB*, strength between brains; *SwB*, strength within brains.

* $p < 0.05$; ** $p < 0.01$; *** $p < 0.001$.

(see Figure 2 for details). The other three GTA measures (*SwB*, *CC*, and E_{local}) in the theta, alpha, and partly also in the beta band, reflecting local processes and processes within the brains, were higher during MU than during AP, especially in the QUA group (see Figure 3 and Table 1 for details). As common HBN analyses cannot provide information on which relationships (Q–Q, P–P, or Q–P) play a more important role, dual analyses were conducted to clarify this issue.

Dual HBN topology

Results of a three-way repeated measures ANOVAs with a between-subject factor Group (Q–Q, P–P, and Q–P) and a within-subject factors Condition (MU vs. AP) and Site (F, C, P, LT, and RT) for the six GTA

measures are presented in Table 2. All main effects were significant for all topology measures in all frequency bands, with the exception of the between-brain strength (*SbB*), showing significant differences only in the delta frequency band. The Group-by-Condition interaction was also mostly significant (with some exceptions) for all frequency ranges. The main effects of the factors Group and Condition and their interaction for the six topology measures at the delta frequency are shown in Figure 4. Results of the other frequency bands can be found in the [Supplementary Materials](#). It can be seen that in practically all cases, the strength (within and between brains), *CC*, and efficiency (local and global) were higher and *CPL* correspondingly shorter for Q–Q pairs or dual networks and lowest (longest in the case of *CPL*) for P–P dual networks. The topology indices for the Q–P pairs or dual networks lay in between.

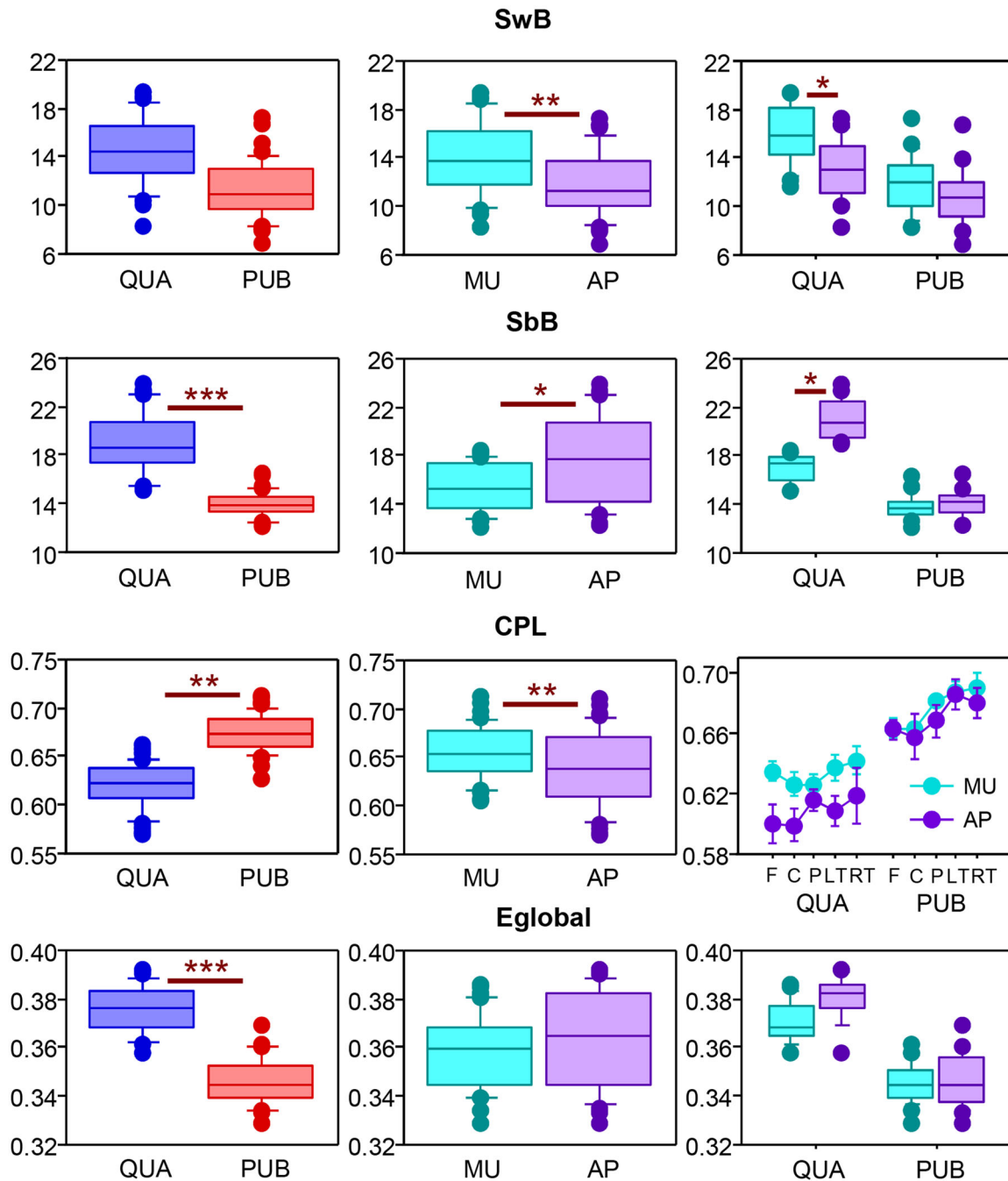


FIGURE 2 ANOVA results for the *common* HBN indices in the delta frequency band. Main effects of the factors Group (QUA vs. PUB) and Condition (MU vs. AP) and their interaction are presented as box plots. Abbreviations: AP, applause; CPL, characteristic path length; E_{global} , global efficiency; MU, music condition; PUB, public audience; QUA, quartet; *SbB*, strength between brains; *SwB*, strength within brains. * $p < 0.05$; ** $p < 0.01$; *** $p < 0.001$.

Relationships between guitar sound structures and the common HBN topology

The results of these analyses at the 99% significance level ($p < 0.01$) are presented in Figure 5. As can be seen, R and GC were expectedly high between guitar sounds (the first four nodes in the matrices indicated by red stripes and red circles in the connectivity maps), indicating relatively similar MSDs of guitar sounds. Moreover, as shown by GC ,

there are directional associations between the sounds of the four guitarists, indicating directional influences between them. The correlation between participants' NTDs was relatively high for SwB and especially for E_{local} , while the correlation between MSDs and NTDs was very low and mostly nonsignificant. However, causal associations between MSDs and NTDs indicated by GC were relatively high (especially for SwB), indicating directional influences of musical and brain structures on each other (see Figure 5 for details). Furthermore, we conducted

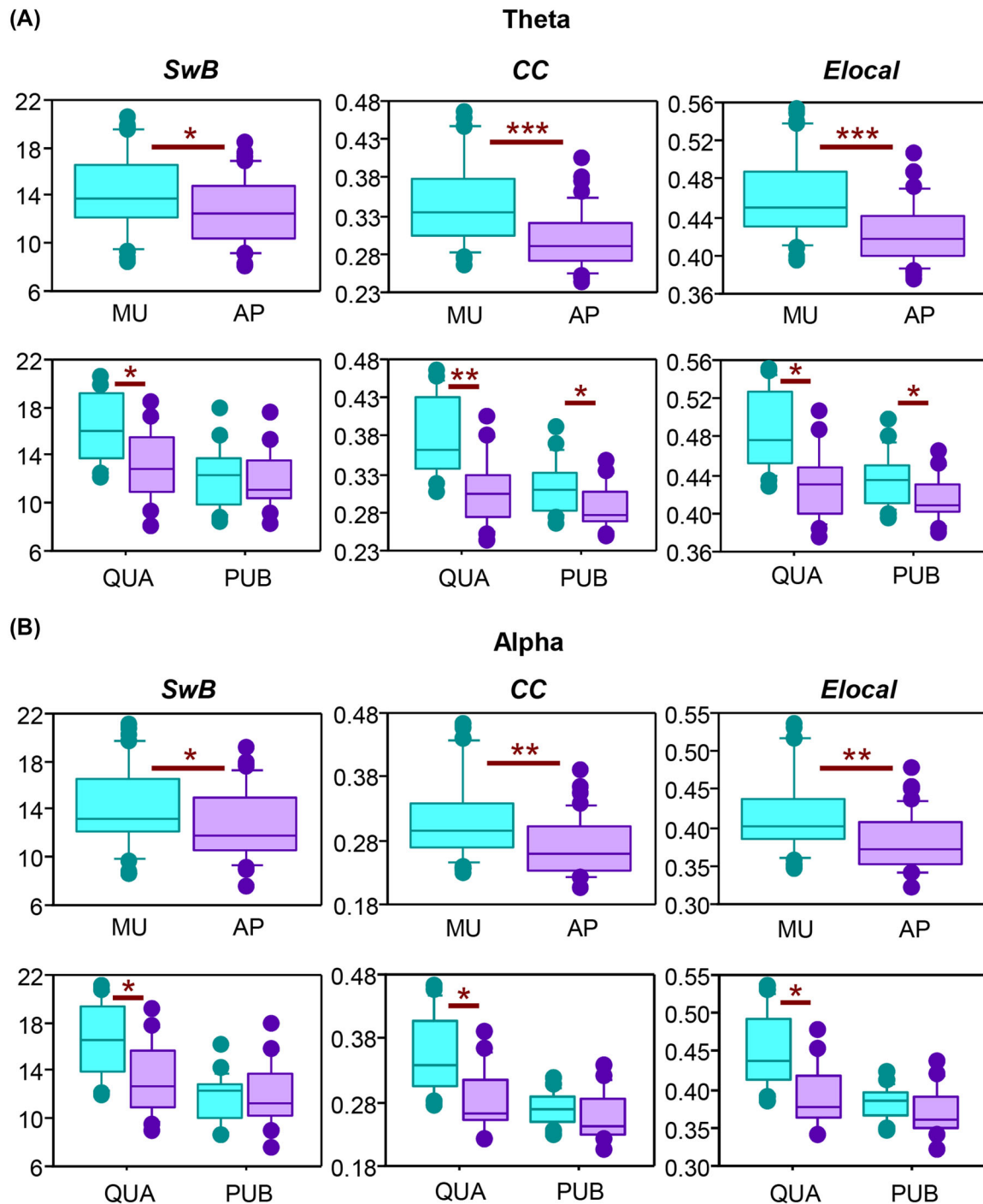


FIGURE 3 ANOVA results for the common HBN indices in the theta and alpha frequency bands. (A) Results for the theta frequency band. (B) Results for the alpha frequency band. Main effects of the factors Group (QUA vs. PUB) and Condition (MU vs. AP) and their interaction are presented as box plots. Abbreviations: AP, applause; CC, clustering coefficient; E_{local} , local efficiency; MU, music condition; PUB, public audience; QUA, quartet; SwB, strength within brains. * $p < 0.05$; ** $p < 0.01$; *** $p < 0.001$.

the same analyses for each piece of music separately, which yielded approximately similar results (see Figures S6–S8).

Modular organization of the common HBNs and its stability

Figure 6 displays intra- and interbrain connectivity and corresponding strength distributions of an exemplary HBN. The color in the connec-

tivity maps on the left indicates the module affinity. All four modules are hyperbrain modules or communities, comprising nodes across several brains. On the right, the distribution of the connectivity strengths within and between brains for each participant (guitarists: A, B, C, and D; audience: E, F, G, and H) and an average across all participants (in the middle) are presented. Dynamic changes of modularity structures in real-time are demonstrated in Video S2. Figure 7A shows similarity matrices determined by MI between all community structures within

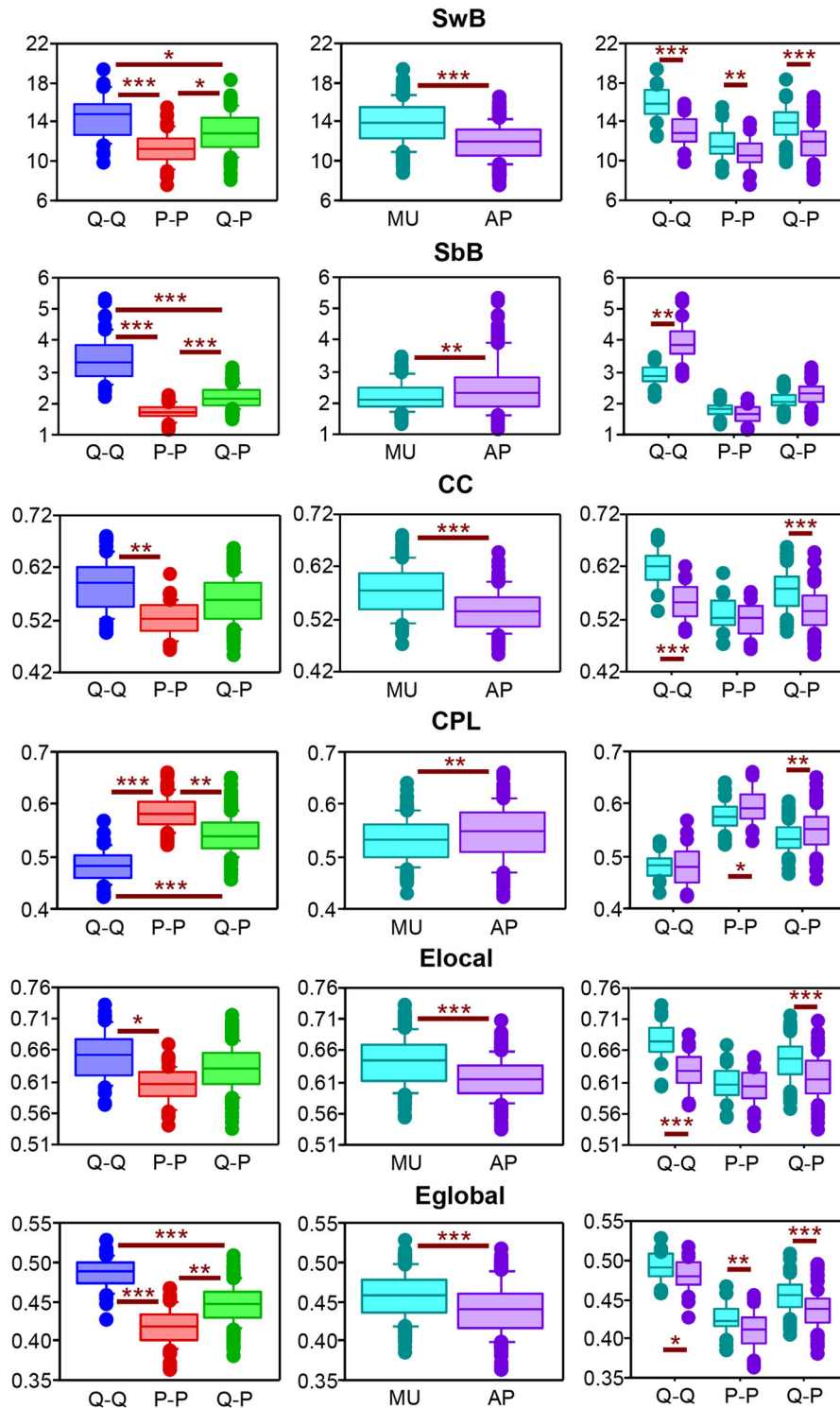


FIGURE 4 ANOVA results for the *dual* HBN indices in the delta frequency band. Main effects of the factors Group (Q-Q, Q-P, and P-P) and Condition (MU vs. AP) and their interaction are presented in a form of the box plots. Abbreviations: AP, applause; CC, clustering coefficient; CPL, characteristic path length; E_{global} , global efficiency; E_{local} , local efficiency; MU, music condition; P-P, public-public dual networks; Q-P, quartet-public dual networks; Q-Q, quartet-quartet dual networks; *SbB*, strength between brains; *SwB*, strength within brains. * $p < 0.05$; ** $p < 0.01$; *** $p < 0.001$.

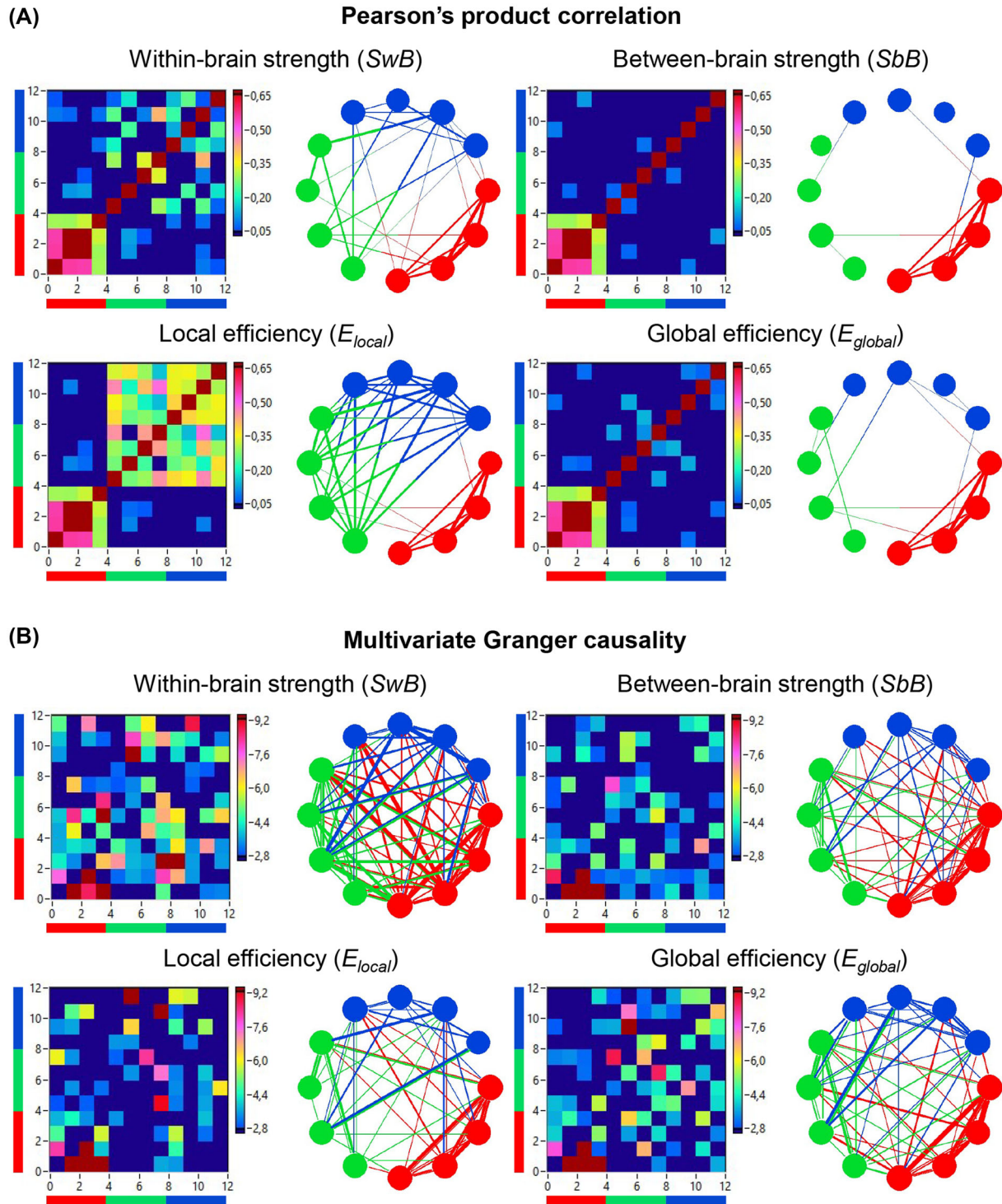


FIGURE 5 Linear and directional relationships between MSD and NTD indices. (A) Linear relationships indicated by Pearson's product correlation. (B) Directional relationships indicated by multivariate Granger causality. The relationships are presented as matrices or heatmaps and circular connectivity maps. In the heatmaps, the red stripe indicates the guitar sounds (nodes 1–4), the green stripe indicates the guitarists (nodes 5–8), and the blue stripe indicates the audience members (nodes 9–12). Similarly, in the connectivity maps, the four red circles or nodes represent the four guitar sounds, the four green circles represent the four guitarists' brains, and the four blue circles represent the four audience members' brains. The linear relationships are symmetric and the directional relationships are asymmetric. The direction of the links is coded by color. Note that the links in the directional connectivity maps are either unidirectional or bidirectional.

TABLE 2 Significant ANOVA results for the dual hyperbrain network indices across the four frequency bands.

Factors	DF	Delta		Theta		Alpha		Beta	
		F value	η^2	F value	η^2	F value	η^2	F value	η^2
<i>SwB</i>									
G	2,25	9.66***	0.44	5.2*	0.29	6.07**	0.33	7.32**	0.37
C	1,25	176.73***	0.88	8.68***	0.76	58.97***	0.70	17.61***	0.41
S	4,100	95.42***	0.79	127.85***	0.84	99.39***	0.80	79.54***	0.76
G × C	2,25	9.32***	0.43	15.44***	0.55	17.49***	0.58	10.96***	0.47
C × S	4,100	n.s.		4.81*	0.16	6.75**	0.21	6.57**	0.21
<i>SbB</i>									
G	2,25	226.7***	0.95	n.s.		n.s.		n.s.	
C	1,25	13.5***	0.35	n.s.		n.s.		n.s.	
S	4,100	10.25***	0.29	n.s.		n.s.		n.s.	
G × C	2,25	10.98***	0.47	n.s.		n.s.		n.s.	
G × S	8,100	4.44***	0.26	n.s.		n.s.		n.s.	
C × S	4,100	7.53***	0.23	n.s.		n.s.		n.s.	
<i>CC</i>									
G	2,25	5.83**	0.32	5.04*	0.29	6.69**	0.35	7.31**	0.37
C	1,25	68.21***	0.73	121.6***	0.83	85.63***	0.77	24.05***	0.49
S	4,100	25.99***	0.51	55.63***	0.69	53.21***	0.68	50.51***	0.67
G × C	2,25	9.41***	0.43	16.86***	0.57	21.46***	0.63	14.29***	0.53
<i>CPL</i>									
G	2,25	24.52***	0.66	5.59**	0.31	6.20**	0.33	8.50**	0.41
C	1,25	8.43**	0.25	28.01***	0.53	29.35***	0.54	13.23***	0.35
S	4,100	95.18***	0.79	131.38***	0.84	91.48***	0.79	66.33***	0.73
G × C	2,25	n.s.		4.53*	0.27	6.78**	0.35	7.82**	0.39
C × S	4,100	n.s.		n.s.		4.08*	0.14	7.17**	0.22
G × C × S	8,100	3.34**	0.21	n.s.		n.s.		n.s.	
<i>E_{local}</i>									
G	2,25	5.23*	0.30	4.81*	0.28	6.75**	0.35	7.80**	0.38
C	1,25	52.92***	0.68	126.0***	0.84	97.0***	0.80	24.62***	0.50
S	4,100	48.32***	0.66	70.2***	0.74	62.14***	0.71	56.85***	0.70
G × C	2,25	7.36**	0.37	16.27***	0.57	23.69***	0.66	15.03***	0.55
<i>E_{global}</i>									
G	2,25	32.78***	0.72	5.68**	0.31	6.01**	0.33	8.32**	0.40
C	1,25	42.35***	0.63	59.78***	0.71	52.34***	0.68	16.77***	0.40
S	4,100	95.04***	0.79	133.42***	0.84	97.02***	0.80	73.99***	0.75
G × C	2,25	n.s.		10.49***	0.46	12.71***	0.50	9.81***	0.44
C × S	4,100	n.s.		3.49*	0.12	5.27*	0.17	5.97*	0.19

Abbreviations: C, Condition; CC, clustering coefficient; CPL, characteristic path length; DF, degrees of freedom; E_{global} , global efficiency; E_{local} , local efficiency; G, Group; n.s., nonsignificant; S, Site; *SbB*, strength between brains; *SwB*, strength within brains.

* $p < 0.05$; ** $p < 0.01$; *** $p < 0.001$.

the three music pieces and during the applause. The *MI* values between one time window and all others (a row in the similarity matrix) were averaged, indicating the similarity of community structures of each time window to all others. Statistical evaluation of these vectors or time series (shown in Figure 7A under the similarity matrices) by paired

t-test showed the significantly lowest similarity during applause in comparison to music conditions (all $ps < 0.001$, Bonferroni-corrected). As shown in Figure 7B, there were also significant differences between music pieces, indicating different similarity or stability of community structures within these pieces (all $ps < 0.001$). We also calculated

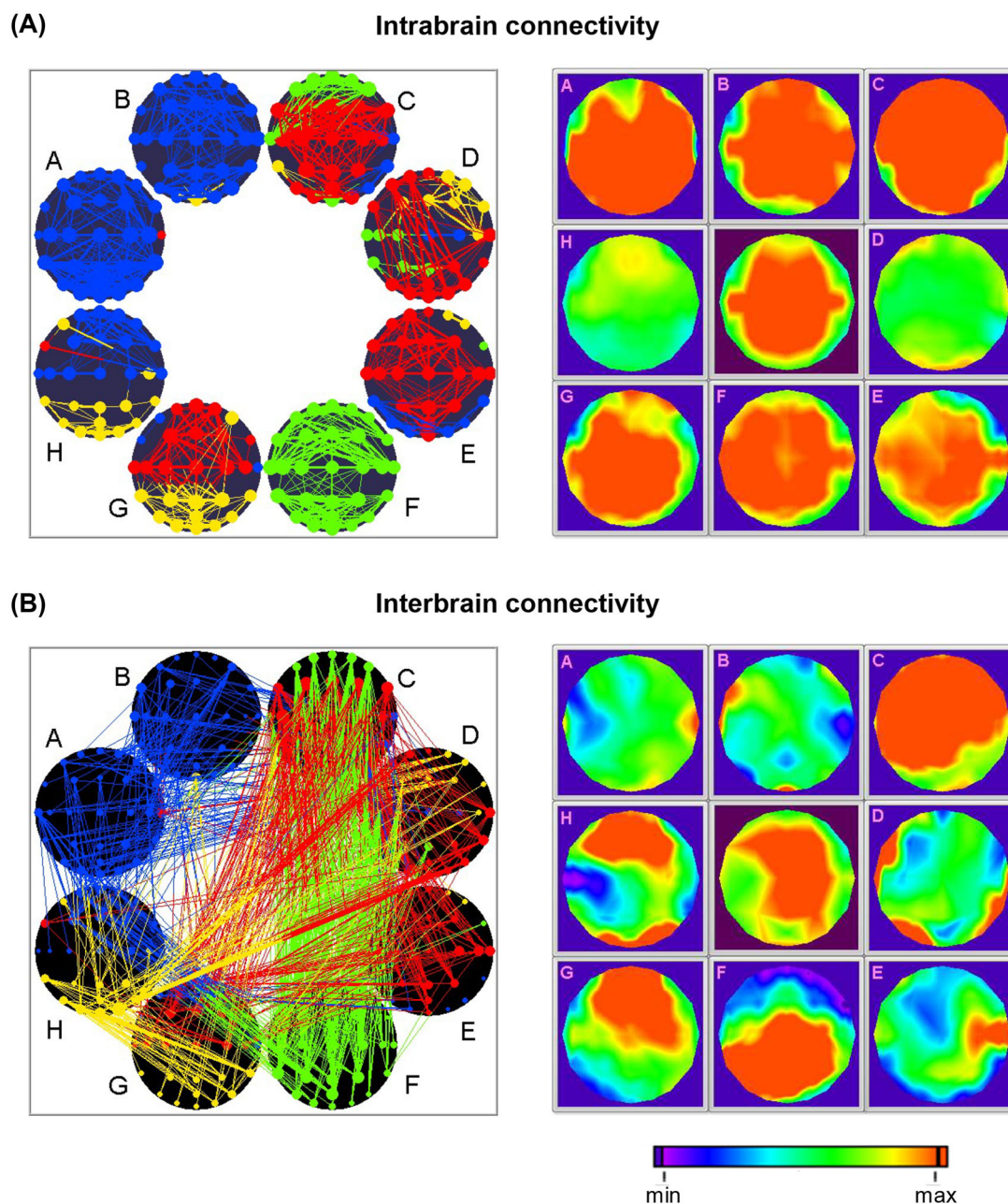


FIGURE 6 Exemplary representation of the hyperbrain modularity or community structure with intra- and interbrain connectivity. (A) Within-brain connectivity maps and topological distribution of strengths within the eight brains. (B) Between-brain connectivity maps and topological distribution of strengths for the between-brain connections. The strength of the nodes (sum of all outgoing connections) in the brain connectivity maps is coded by circle size, and the strength of edges is coded by line thickness. The different modules are coded by color. Please note that only the strongest within- and between-brain connections are displayed. The guitarists' brains are denoted A, B, C, and D, and the audience members' brains are denoted E, F, G, and H.

modularity values, providing a statistic that quantifies the degree to which the network may be subdivided into clearly delineated groups or modules. As shown in Figure 7C, the modularity values show a similar pattern of differences between conditions as the similarity values, with a significantly lowest modularity during applause as compared to music conditions (all $ps < 0.001$). This indicates that the partitioning

of the HBNs into modules or communities was more stable during music conditions than during applause. There were also significant differences between music conditions or pieces (all $ps < 0.01$; see Figure 7C for details). Here, it should be noted that all conditions (also the AP condition) showed high modularity values (more than 0.28), indicating a good partition of HBNs into modules or communities.

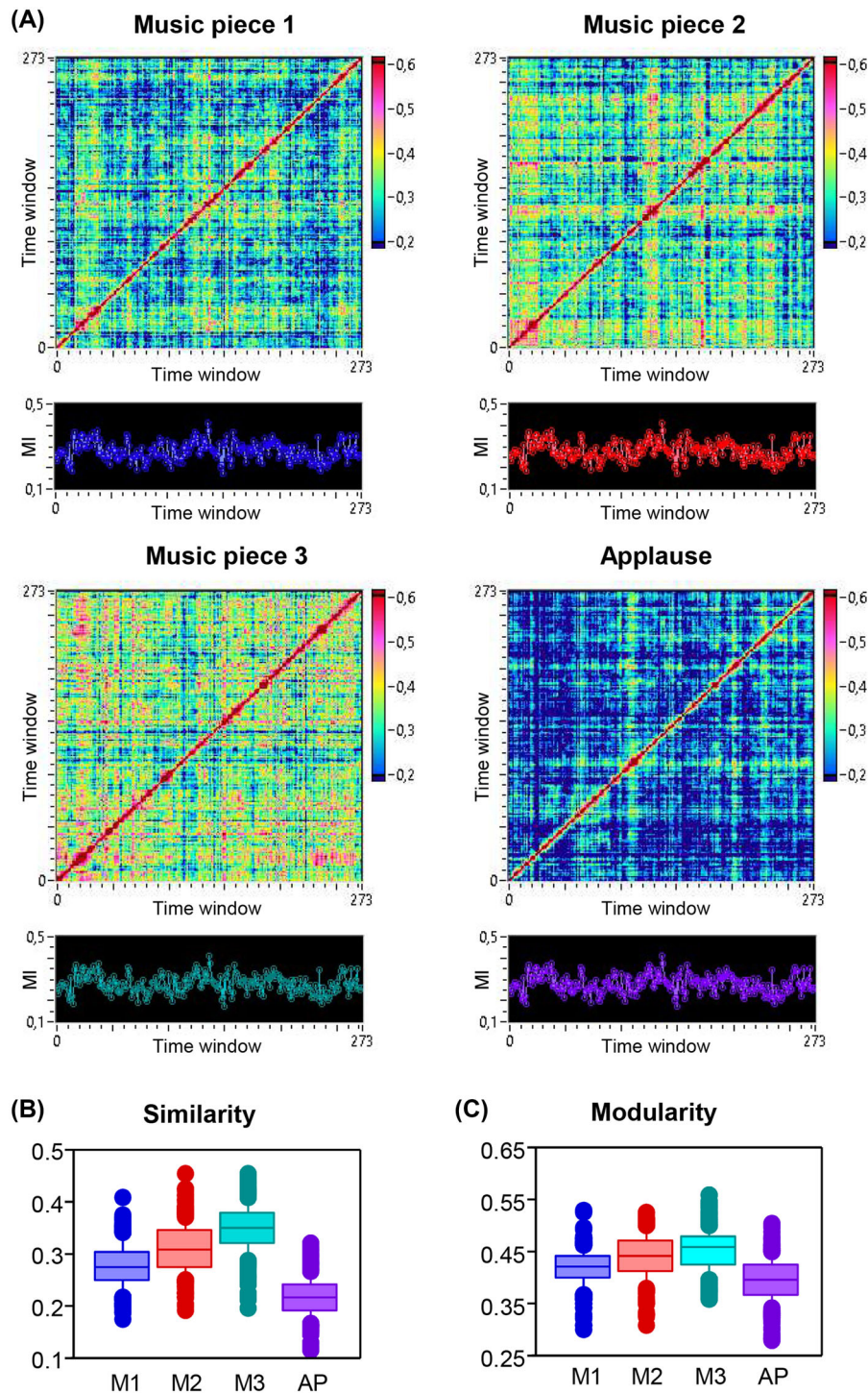


FIGURE 7 Similarity and modularity of community structures within the three music pieces and during applause. (A) Similarity matrices determined by *MI* between all community structures within the three music pieces and during the applause. Community structures were calculated for each time window across three SOIs (273 time windows in total). Under the matrices, mean *MI* values averaged across the rows are presented. (B) Box plots of the mean *MI* values for the three music piece and applause conditions. (C) Box plots of the modularity values for the three music piece and applause conditions. Modularity values were determined for each community structure as a statistic for the degree to which the common HBN may be subdivided into clearly delineated groups or modules. Note that the differences in the similarity (*MI*) and modularity (*Q*) were highly significant ($p < 0.001$) between all four conditions.

DISCUSSION

The primary objective of this study was to investigate the intra- and interbrain dynamics and hyperbrain architecture and dynamics emerging in a quartet of guitarists and the audience during a concert. The main findings are that: (1) practically all GTA measures in the common and especially in the dual HBNs showed significant differences between the quartet and audience members during music performance and the applause, which were also frequency-specific in the common HBNs; (2) in the delta band, S_{wB} was higher and S_{bB} was lower in the MU as compared to the AP condition, both mostly in the QUA group and for the Q–Q relations; (3) guitar sounds not only correlated with, or predicted each other, but this correlation or prediction in the Granger sense also concerned guitar–brain and brain–brain relations with respect to the dynamics of corresponding structures; and (4) the HBNs exhibit modular structures with hyperbrain modules or communities, comprising nodes across several brains, and the dynamics of these community structures was much more stable during the music performance than during the applause.

In the *common* HBN analyses, the factor Group was significant for S_{bB} , CPL , and E_{global} (only in the delta band), indicating higher S_{bB} and E_{global} and shorter CPL in the QUA as compared to the PUB group. In contrast, the Condition factor and the Group-by-Condition interaction were significant for S_{wB} , CC , and E_{local} in the theta and alpha frequency ranges, which were higher in the MU than in the AP condition, especially in the QUA group (see Figure 3). This discrepancy indicates that the low frequency (delta band) is responsible for group differences with respect to the *interbrain* connectivity and HBN *integration*, whereas the faster theta and alpha frequencies support condition differences with respect to the *intrabrain* connectivity and HBN *segregation*. Thus, the common HBNs have two different modes (i.e., *global* with enhanced interbrain connectivity and network integration, and *local* with strong intrabrain connectivity and network segregation), which are working at different frequencies with respect to group and condition differences. Interestingly, the factor Condition was also significant for S_{bB} and CPL in the delta band, but in contrast to S_{wB} , S_{bB} was higher and CPL was shorter in the AP as compared to the MU condition. Thus, the delta band is also sensitive to condition differences but in different way than local processes at faster theta and alpha frequencies, which were higher in MU than AP condition. This differentiation for frequency and topology measures or modes (local vs. global) is very interesting and probably characteristic for HBNs with different functional units (e.g., musicians and audience).

As mentioned above, the S_{bB} in the common HBN includes Q–Q and Q–P connections in the case of the QUA group and P–P and Q–P connections in the case of the PUB group. Accordingly, the *dual* HBN analyses, which allowed us to separate these three types of connections (i.e., Q–Q, P–P, and Q–P), showed generally higher S_{bB} (also only in the delta band) in the Q–Q than in the Q–P and P–P groups, and higher S_{bB} in the Q–P than in the P–P group. Like the common HBNs, S_{bB} in the dual HBNs was also lower in the MU than in the AP condition, especially in the Q–Q group. In contrast to this and to the common HBN analyses, CPL in the dual networks was shorter in

the MU than in the AP condition, especially in the Q–P and P–P dual networks. In addition, other GTA measures (S_{wB} , CC , E_{local} , and E_{global}) were highest in the Q–Q and lowest in the P–P groups, and generally higher during the music performance than during the applause, especially in the Q–Q and Q–P dual networks. Moreover, this relationship also holds for other frequency bands (i.e., theta, alpha, and beta). All this suggests that active interaction (making music) evokes stronger connections within and between brains in musicians during a concert than in the audience and changes the topology of the HBNs toward the small-world networks with higher segregation (higher CC and E_{local}) and integration (shorter CPL and higher E_{global}) of neural processes. There is neurophysiological evidence that neural networks generally exhibit “small-world” structures (i.e., high levels of clustering and short path lengths) that support efficient information segregation and integration with low energy and wiring costs as well as a high rate of information transmission and communication.^{35–38} The small-world structure of HBNs suggests a more efficient and effective communication between brains when interaction demands are higher. This confirms the findings made previously in a guitarist quartet¹³ and guitarist duets,^{12,15} which showed small-world properties of the HBNs and an increase in small-worldness with higher frequency. However, it has also been shown that low frequencies (e.g., delta and theta) play an essential role in interbrain dynamics.^{9,10,12,13,15} Interestingly, significant differences between the groups and conditions in the S_{bB} (both in common and dual networks) were found only in the delta band, supporting the previous findings. In EEG hyperscanning studies, it has been shown that an increase in interbrain synchrony in an audience during live music was dependent on emotional pleasure and closeness as well as on the number of people sharing pleasure and its strength.^{22,23} Whether the greater pleasure of musicians than of audience members or a certain degree of asynchrony in the audience during applause or other factors are responsible for the differences in S_{bB} at the delta frequency between musicians and the audience during applause remains to be seen. However, it is obvious that musicians and listeners behave differently during the concert and that this influences the different brain dynamics, which find their expression in the different synchronization patterns and HBN topology dynamics. Moreover, the differentiation for frequency and topology measures or modes (local vs. global) that was demonstrated in the *common* HBN analyses could not be verified for the dual networks. Apparently, this differentiation is characteristic only for larger networks where all connections are taken into account. These (larger) networks use different frequencies for local and global processes depending on the situation (e.g., MU or AP). This very interesting phenomenon clearly requires further sophisticated investigation.

The observed significant correlation between guitar sounds was not surprising, even though the guitarists played different parts of the music. However, the musical structures (MSD) determined by the SSMs were relatively similar and, therefore, showed strong correlations. However, the correlation between the MSD of guitar sounds and the NTD of the guitarists’ and audience members’ brains was relatively low, but did reach the significance level in some cases. Most interestingly, MSD and NTD predicted each other in a Granger sense,

especially in the case of *SwB*, but also in the case of other topology measures. A synchronization between brains and instruments was reported previously.^{8,10,11,26} Here, we show another level of synchrony or prediction, where structures of music (MSD) and brain dynamics (NTD) are related to each other or predict each other, and this concerns not only the guitarists' but also the audience members' brains. In the hyperscanning study on guitarist duets with a directed synchronization measure, it has been shown that the relations between brains and instruments are unidirectional or bidirectional.¹¹ As suggested, "the instrument's sound is a result of the musician's behavior, which is based on sensorimotor synchronization and action. At the same time, this sound influences the behavior of musicians through auditory sensory pathways and is in this sense an actor" (Müller and Lindenberger¹¹). Moreover, the directional coupling from brains to instruments can be considered as an anticipation process, predicting a specific or expected musical structure. As proposed by Keller et al.,² anticipation processes can "facilitate precise rhythmic interpersonal coordination by allowing individuals to plan the timing of their own actions with reference to predictions about the future time course of others' actions." This anticipation process presumably also concerns the audience members, who also showed high GC from their brains to instrument sounds or MSD but also to the NTD of the guitarists' brains. There were also strong (linear) correlations between the NTDs of guitarists and audience members, at least in the case of *SwB* and local efficiency. This may be a result of the brain–brain coupling found in the present study, in addition to the direct effect of music on brains or on the common HBN of the guitarists and the audience. All these relationships, which emerge on different levels of organization (e.g., oscillatory, network-related, etc.), are interconnected and interwoven, and constitute a common construct or superorganism with multilevel dynamics and upward and downward causation (cf. Refs. 19,20,39, and 40). Clearly, further sophisticated research is needed to deepen our understanding of these highly interesting and complex phenomena.

As mentioned above, the HBNs exhibit a modular structure, with hyperbrain modules or communities comprising nodes across several brains. Thus, the hyperbrain modules with the strongest connections between the nodes within the modules must have an important functional meaning (cf. Refs. 19 and 20). These strong connections within the hyperbrain modules are likely important for information transfer between the brains as well as within them, and for simultaneous and probably synchronized firing of neural cells within these brains. It has been suggested that hyperbrain modules can be considered as a prototype of so-called hyperbrain cell assemblies and that hyperbrain cell assemblies that are formed during an interaction should gain precedence during repeated joint activity.¹⁹ Here, we have shown that the hyperbrain community structure is more stable in the music condition than during applause. This can indicate that some hyperbrain cell assemblies or a specific configuration of brain activity are favored during music and occur repeatedly, thus contributing a certain stability to the aforementioned hyperbrain community structures emerging across time. Such recovery of a specific neural activity configuration can be induced via a self-similar musical structure that evokes certain self-similarity in the HBNs or cell assemblies that can

be reinforced or modulated by the emotional pleasure of musicians and audience members.^{41–43} The concept of recurrence is prominent in many disciplines or approaches and is strictly related to the temporal evolution of complex dynamical systems indicating periodic behavior.^{39,44,45} Applause is definitely a periodic and recurrent action but is, presumably, not as well organized as making music or listening to it, which might explain the higher variability (or lower stability) of the hyperbrain community structure across time in the AP as compared to the MU condition.

The results of this study may have implications for real-world music playing and group interaction. As proposed by Hasson and Frith,⁴⁶ "...interactions with other members of a group can fundamentally shape the way we behave in the world, and alignment is a ubiquitous feature of such interactions." Our study shows that such an alignment presupposes different types of synchronization and network dynamics with different modes for different parts of the system or HBN (e.g., musicians and/or audience), depending on the situation (music making or applause). As noted by D'Ausilio et al.,³ "group-level musical coordination can be considered as a microcosm of social interaction. Individual musicians function as processing units within a complex dynamical system (the ensemble) whose goal is to communicate musical meaning (which is aesthetic and affective in nature) to an audience. Information flows simultaneously to and from each unit, and the system as a whole relies upon predictive models and adaptive mechanisms to meet the real-time demands of interpersonal coordination. As in more general forms of social interaction, co-performers behave in complex but formalized (rule-based) ways that are constrained by the tools they use (musical instruments), conventions (genre-specific performance styles and leader–follower roles), and often a script (the musical score)." The results of our study confirm this view and suggest some further implications in terms of HBN dynamics and their relations to instruments or instrument sounds during a real concert.

LIMITATIONS

The present study has limitations and leaves room for questions to be addressed in future research. First, the sample size of our study was small, which has implications for generalizability. However, the main patterns of HBN connectivity and network organization were comparable across different musical pieces and frequency bands. Second, our analyses were limited to phase synchronization within single-frequency bands. Cross-frequency coupling is likely to provide further information about functionally relevant network properties and NTD.^{19,47,48} Thus, further sophisticated research is needed to shed light on neuronal mechanisms of concert interaction and behavior.

CONCLUSION

Our results showed that intra- and interbrain synchrony and resulting HBN topology differ in the quartet and audience members during the music performance and applause in a concert of a quartet. The

HBN topology and MSD of guitar sounds showed specific guitar–brain, guitar–guitar, and brain–brain directional associations, suggesting multilevel dynamics with upward and downward causation. The HBN architecture exhibits a modular organization with hyperbrain modules or communities that are more stable during music performance than during applause. Thus, observation of dynamic changes in synchronization and network architecture seems to be essential to achieve a profound understanding of group dynamics and social interaction.

AUTHOR CONTRIBUTIONS

V.M. and U.L. designed the study. V.M. acquired, prepared, and analyzed the data. V.M. and U.L. discussed the results. V.M. wrote the article. V.M. and U.L. read and approved the final version of the manuscript.

ACKNOWLEDGMENTS

We thank the guitarists of the Cuarteto Apasionado for participation in the study. Our greatest thanks go to Johanna Sanger, who was involved in the designing and conducting the study from the very beginning. The authors are grateful to Bibiana Klempova, Lissa Mapouyat, Daphna Raz, Jakob Volhard, Christine Wolter, and Anna Wurtz for technical assistance and for carrying out the experimental part of the study. We thank Zurab Schera and Berndt Wischnewski for data acquisition and software assistance. The authors thank Julia Delius for language assistance. This research was supported by the Max Planck Society.

Open access funding enabled and organized by Projekt DEAL.

COMPETING INTERESTS

The authors declare no competing interests.

PEER REVIEW

The peer review history for this article is available at <https://publons.com/publon/10.1111/nyas.14987>

REFERENCES

- Nozaradan, S., Peretz, I., & Keller, P. E. (2016). Individual differences in rhythmic cortical entrainment correlate with predictive behavior in sensorimotor synchronization. *Scientific Reports*, 6, 20612.
- Keller, P. E., Novembre, G., & Hove, M. J. (2014). Rhythm in joint action: Psychological and neurophysiological mechanisms for real-time interpersonal coordination. *Philosophical Transactions of the Royal Society B*, 369, 20130394.
- D'Ausilio, A., Novembre, G., Fadiga, L., & Keller, P. E. (2015). What can music tell us about social interaction? *Trends in Cognitive Sciences*, 19, 111–114.
- Badino, L., D'ausilio, A., Glowinski, D., Camurri, A., & Fadiga, L. (2014). Sensorimotor communication in professional quartets. *Neuropsychologia*, 55, 98–104.
- Keller, P. E., Novembre, G., & Loehr, J. (2016). Musical ensemble performance: Representing self, other, and joint action outcomes. In E. Cross & O. Sukhinder (Eds.), *Shared representations: Sensorimotor foundations of social life* (pp. 280–310). Cambridge: Cambridge University Press.
- Acquadro, M. A. S., Congedo, M., & De Ridder, D. (2016). Music performance as an experimental approach to hyperscanning studies. *Frontiers in Human Neuroscience*, 10, 242.
- Sanger, J., Muller, V., & Lindenberger, U. (2013). Directionality in hyperbrain networks discriminates between leaders and followers in guitar duets. *Frontiers in Human Neuroscience*, 7, 234.
- Gugnowska, K., Novembre, G., Kohler, N., Villringer, A., Keller, P. E., & Sammler, D. (2022). Endogenous sources of interbrain synchrony in duetting pianists. *Cerebral Cortex*, 32, 4110–4127.
- Lindenberger, U., Li, S.-C., Gruber, W., & Muller, V. (2009). Brains swinging in concert: Cortical phase synchronization while playing guitar. *BMC Neuroscience [Electronic Resource]*, 10, 22.
- Muller, V., & Lindenberger, U. (2022). Probing associations between interbrain synchronization and interpersonal action coordination during guitar playing. *Annals of the New York Academy of Sciences*, 1507, 146–161.
- Muller, V., & Lindenberger, U. (2019). Dynamic orchestration of brains and instruments during free guitar improvisation. *Frontiers in Integrative Neuroscience*, 13, 50.
- Muller, V., Sanger, J., & Lindenberger, U. (2013). Intra- and inter-brain synchronization during musical improvisation on the guitar. *PLoS ONE*, 8, e73852.
- Muller, V., Sanger, J., & Lindenberger, U. (2018). Hyperbrain network properties of guitarists playing in quartet. *Annals of the New York Academy of Sciences*, 1423, 198–210.
- Sanger, J., Lindenberger, U., & Muller, V. (2011). Interactive brains, social minds. *Communicative & Integrative Biology*, 4, 655–663.
- Sanger, J., Muller, V., & Lindenberger, U. (2012). Intra- and interbrain synchronization and network properties when playing guitar in duets. *Frontiers in Human Neuroscience*, 6, 312.
- Czeszumski, A., Eustergerling, S., Lang, A., Menrath, D., Gerstenberger, M., Schuberth, S., Schreiber, F., Rendon, Z. Z., & Konig, P. (2020). Hyper-scanning: A valid method to study neural inter-brain underpinnings of social interaction. *Frontiers in Human Neuroscience*, 14, 39.
- Frith, C. D., & Frith, U. (2007). Social cognition in humans. *Current Biology*, 17, R724–R732.
- Hari, R., & Kujala, M. V. (2009). Brain basis of human social interaction: From concepts to brain imaging. *Physiological Reviews*, 89, 453–479.
- Muller, V. (2022). Neural synchrony and network dynamics in social interaction: A hyper-brain cell assembly hypothesis. *Frontiers in Human Neuroscience*, 16, 848026.
- Muller, V., Ohstrom, K.-R. P., & Lindenberger, U. (2021). Interactive brains, social minds: Neural and physiological mechanisms of interpersonal action coordination. *Neuroscience and Biobehavioral Reviews*, 128, 661–677.
- Thompson, E., & Varela, F. J. (2001). Radical embodiment: Neural dynamics and consciousness. *Trends in Cognitive Sciences*, 5, 418–425.
- Chabin, T., Gabriel, D., Comte, A., Haffen, E., Moulin, T., & Pazart, L. (2022). Interbrain emotional connection during music performances is driven by physical proximity and individual traits. *Annals of the New York Academy of Sciences*, 1508, 178–195.
- Chabin, T., Gabriel, D., Comte, A., & Pazart, L. (2022). Audience inter-brain synchrony during live music is shaped by both the number of people sharing pleasure and the strength of this pleasure. *Frontiers in Human Neuroscience*, 16, 855778.
- Neda, Z., Ravasz, E., Vicsek, T., & Barabasi, A.-L. (2000). The sound of many hands clapping. *Nature*, 403, 849–850.
- Neda, Z., Ravasz, E., Vicsek, T., Brechet, Y., & Barabasi, A. L. (2000). Physics of the rhythmic applause. *Physical Review E*, 61, 6987–6992.
- Zamm, A., Debener, S., Bauer, A.-K. R., Bleichner, M. G., Demos, A. P., & Palmer, C. (2018). Amplitude envelope correlations measure synchronous cortical oscillations in performing musicians. *Annals of the New York Academy of Sciences*, 1423, 251–263.
- Muller, M. (2021). *Fundamentals of music processing*. Springer International Publishing.
- Vigario, R. N. (1997). Extraction of ocular artefacts from EEG using independent component analysis. *Electroencephalography and Clinical Neurophysiology*, 103, 395–404.
- Muller, V., Perdikis, D., Von Oertzen, T., Sleimen-Malkoun, R., Jirsa, V., & Lindenberger, U. (2016). Structure and topology dynamics of

- hyper-frequency networks during rest and auditory oddball performance. *Frontiers in Computational Neuroscience*, 10, 108.
30. Newman, M. E. J. (2004). Analysis of weighted networks. *Physical Review E*, 70, 1–9.
 31. Newman, M. E. J. (2006). Finding community structure in networks using the eigenvectors of matrices. *Physical Review E*, 74, 036104.
 32. Rubinov, M., & Sporns, O. (2010). Complex network measures of brain connectivity: Uses and interpretations. *Neuroimage*, 52, 1059–1069.
 33. Strehl, A., & Ghosh, J. (2003). Cluster ensembles – A knowledge reuse framework for combining multiple partitions. *Journal of Machine Learning Research*, 3, 583–617.
 34. Vinh, N. X., Epps, J., & Bailey, J. (2010). Information theoretic measures for clusterings comparison: Variants, properties, normalization and correction for chance. *Journal of Machine Learning Research*, 11, 2837–2854.
 35. Achard, S., Salvador, R., Whitcher, B., Suckling, J., & Bullmore, E. (2006). A resilient, low-frequency, small-world human brain functional network with highly connected association cortical hubs. *Journal of Neuroscience*, 26, 63–72.
 36. Bassett, D. S., & Bullmore, E. (2006). Small-world brain networks. *Neuroscience*, 12, 512–523.
 37. Telesford, Q. K., Joyce, K. E., Hayasaka, S., Burdette, J. H., & Laurienti, P. J. (2011). The ubiquity of small-world networks. *Brain Connectivity*, 1, 367–375.
 38. Watts, D. J., & Strogatz, S. H. (1998). Collective dynamics of “small-world” networks. *Nature*, 393, 440–442.
 39. Buzsáki, G. (2006). *Rhythms of the brain*. Oxford: Oxford University Press.
 40. Haken, H. (1983). *Synergetics: An introduction: Nonequilibrium phase transitions and self-organization in physics, chemistry*. Berlin: Springer-Verlag.
 41. Blood, A. J., & Zatorre, R. J. (2001). Intensely pleasurable responses to music correlate with activity in brain regions implicated in reward and emotion. *Proceedings of the National Academy of Sciences of the United States of America*, 98, 11818–11823.
 42. Ferreri, L., Mas-Herrero, E., Zatorre, R. J., Ripollés, P., Gomez-Andres, A., Alicart, H., Olivé, G., Marco-Pallarés, J., Antonijoan, R. M., Valle, M., Riba, J., & Rodriguez-Fornells, A. (2019). Dopamine modulates the reward experiences elicited by music. *Proceedings of the National Academy of Sciences of the United States of America*, 116, 3793–3798.
 43. Salimpoor, V. N., Benovoy, M., Larcher, K., Dagher, A., & Zatorre, R. J. (2011). Anatomically distinct dopamine release during anticipation and experience of peak emotion to music. *Nature Neuroscience*, 14, 257–262.
 44. Buzsáki, G. (2010). Neural syntax: Cell assemblies, synapse ensembles, and readers. *Neuron*, 68, 362–385.
 45. Buzsáki, G. (2019). *The brain from inside out*. New York: Oxford University Press.
 46. Hasson, U., & Frith, C. D. (2016). Mirroring and beyond: Coupled dynamics as a generalized framework for modelling social interactions. *Philosophical Transactions of the Royal Society B*, 371, 20150366.
 47. Jirsa, V., & Müller, V. (2013). Cross-frequency coupling in real and virtual brain networks. *Frontiers in Computational Neuroscience*, 7, 78.
 48. Müller, V., & Lindenberger, U. (2014). Hyper-brain networks support romantic kissing in humans. *PLoS ONE*, 9, e112080.

SUPPORTING INFORMATION

Additional supporting information can be found online in the Supporting Information section at the end of this article.

How to cite this article: Müller, V., & Lindenberger, U. (2023).

Intra- and interbrain synchrony and hyperbrain network dynamics of a guitarist quartet and its audience during a concert. *Ann NY Acad Sci.*, 1523, 74–90.

<https://doi.org/10.1111/nyas.14987>